J Med Syst (2015) 39: 128
DOI 10.1007/s10916-015-0316-1

PATIENT FACING SYSTEMS

Hybrid Features and Mediods Classification based Robust Segmentation of Blood Vessels

Amna Waheed[1] · M. Usman Akram[1] · Shehzad Khalid[2] · Zahra Waheed[1] · Muazzam A Khan[1] · Arslan Shaukat[1]

Received: 5 May 2015 / Accepted: 5 August 2015 / Published online: 26 August 2015

Abstract Retinal blood vessels are the source to provide oxygen and nutrition to retina and any change in the normal structure may lead to different retinal abnormalities. Automated detection of vascular structure is very important while designing a computer aided diagnostic system for retinal diseases. Most popular methods for vessel segmentation are based on matched filters and Gabor wavelets which give good response against blood vessels. One major drawback in these techniques is that they also give strong response for lesion (exudates, hemorrhages) boundaries which give rise to false vessels. These false vessels may lead to incorrect detection of vascular changes. In this paper, we propose a new hybrid feature set along with new classification technique for accurate detection of blood vessels. The main motivation is to lower the false positives especially from retinal images with severe disease level. A novel region based hybrid feature set is presented for proper discrimination between true and false vessels. A new modified m-mediods based classification is also presented which uses most discriminating features to categorize vessel regions into true and false vessels. The evaluation of proposed system is done thoroughly on publicly available databases along with a locally gathered database with images of advanced level of retinal diseases. The results demonstrate the validity of the proposed system as compared to existing state of the art techniques.

Keywords Ocular diseases · Shape and intensity based features · Mediods based classification · False vessels · Lesions

This article is part of the Topical Collection on *Patient Facing Systems*

✉ M. Usman Akram
usmakram@gmail.com

Shehzad Khalid
shehzad_khalid@hotmail.com

[1] Department of Computer Engineering College of Electrical & Mechanical Engineering, National University of Sciences & Technology, Rawalpindi, Pakistan

[2] Computer & Software Engineering Department, Bahria University, Islamabad, Pakistan

Introduction

Different clinical studies on medical imaging have highlighted that many diseases i.e. diabetes, hypertension, malaria etc screen themselves in human retina [1, 2]. Blood vessels, fovea, optic disc and macula are the normal retinal features and any retinal abnormality may cause variation in normal structure of these features. Blood vessels capture the most significant information about vascular changes made by different ophthalmological disorders [3]. Diabetic Retinopathy (DR) and Hypertensive Retinopathy (HR) are micro vascular complications of diabetes and hypertension and cause blindness if not treated timely. DR is further classified into two broad stages i.e. Non-Proliferative Diabetic Retinopathy (NPDR) and Proliferative Diabetic Retinopathy (PDR) [4–6]. DR causes the appearance of many abnormal structures such as Soft and Hard exudates, hemorrhages and growth of some new abnormal vasculature in human retina.

Digital fundus images are acquired through fundus camera which can be used for computerized detection of many retinal diseases [1]. Fundus imaging is being tremendously used to monitor and detect retinal abnormality [2]. Figure 1

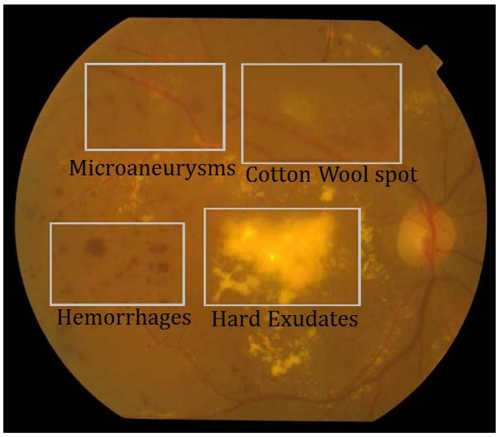

Fig. 1 Digital retinal image with distinctive signs of retinal diseases

shows digital retinal image with abnormal structures due to retinal diseases. These abnormal structures appear as different spots with strong and fuzzy edges.

Computer-aided diagnosis of retinal images plays an important role in retinal analysis, screening and detection of many ocular diseases [7]. Automated retinal analysis is required for timely detection of many ocular diseases to avoid the risk of vision impairments. Most of the automatic and semi-automatic methods to analyze the retinal vasculature rely on a vessel segmentation [7]. Automated segmentation of blood vessels is the pre-requisite of many computer-aided diagnosis systems in the screening process of ophthalmological disorders [7]. Vessel segmentation is a complex problem even in healthy retinal images and becomes even more complicated and crucial when images start to show pathological signs such as exudates, hemorrhages etc. Moreover, existence of other anatomical features in retina disrupts automated mechanism of blood vessels segmentation. There are many other factors as well which makes segmentation even harder such as poor illumination, variant intensities and widths of blood vessels etc. Therefore, automated segmentation of retinal vasculature is one optimal way to extract blood vessels in the presence of lesions and its effects. It would be valuable for the early detection and characterization of changes due to ocular diseases.

Rest of the paper is structured as follows, Section "Related work" discusses various previous techniques on vessel segmentation. Section "Proposed method" explains proposed methodology and results are given in Section "Experimental results" while Section "Conclusion" which is last section of paper has conclusion and discussion.

Related work

A significant amount of work has been done on vessel segmentation over the past few years. Soares et al. [8] developed a retinal vasculature segmentation technique combining 2D Gabor Wavelet and supervised classification. The Bayesian classifier using Gaussian Mixture Model (GMM) was employed to classify each pixel as vessel or non-vessel. This method was evaluated on DRIVE and STARE databases but this method didn't cater the presence of pathological signs in segmentation. Raja et al. [9] came up with supervised technique with local binary patterns and texture features fed to SVM classifier for segmentation of blood vessels. The proposed methodology was implemented on STARE and DRIVE databases. This method produced poor segmentation results in the case of diseased retinal images. An effective approach for retinal vessel segmentation was proposed by Holbura et al. [10]. The proposed approach used the combination of two powerful machine learning classifiers i.e. SVM and Neural Networks with the features of Intensity of Green Channel (IGC),

Table 1 Summary of related work

Authors	Year	Category	Databases	Performance Measures
Imani et al. [20]	2015	Unsupervised	STARE,DRIVE	TPR, TNR, ACC
Wang et al. [11]	2015	Supervised	STARE, DRIVE	TPR, TNR, ACC
Shruthi et al. [18]	2014	Supervised	Own dataset	–
Aramesh et al. [14]	2014	Unsupervised	DRIVE	TPR, TNR, ACC
Emary et al. [12]	2014	Unsupervised	STARE, DRIVE	TPR, TNR, ACC
Raja et al. [9]	2014	Supervised	STARE, DRIVE	TPR, TNR, ACC
Asad et al. [13]	2013	Unsupervised	DRIVE	TPR, TNR, ACC
Tagore et al. [16]	2013	Unsupervised	STARE,DRIVE	ACC
Akram et al. [19]	2013	Supervised	STARE,DRIVE, DIARETDB, MESSIDOR	TPR, TNR, ACC
Nyuyen et al. [15]	2012	Unsupervised	STARE,DRIVE,REVIEW	ACC
Holbara et al. [10]	2012	Supervised	DRIVE	ACC
Fraz et al. [2]	2012	Supervised	STARE, DRIVE, CHASEDB1	TPR, TNR, ACC
Soares et al. [8]	2006	Supervised	STARE, DRIVE	ACC

Table 2 Image wise vessel segmentation results for DRIVE database

	OBSERVER 1			OBSERVER 2		
IMG	TPR	TNR	ACC	TPR	TNR	ACC
1	86.60	96.65	95.75	87.14	96.99	96.13
2	84.49	97.65	96.30	84.78	98.07	96.74
3	79.35	96.93	95.18	84.45	97.06	95.94
4	79.54	98.06	96.36	81.58	98.30	96.83
5	77.91	98.19	96.29	84.73	98.25	97.16
6	79.41	97.13	95.41	80.51	97.50	95.92
7	78.92	97.72	96.00	87.44	97.17	96.47
8	80.71	96.26	94.92	87.17	95.68	95.12
9	82.21	97.06	95.86	80.72	97.40	96.06
10	80.16	98.00	96.53	85.10	98.05	97.12
11	80.25	97.11	95.60	84.63	97.41	96.35
12	84.03	97.11	95.98	86.28	97.23	96.35
13	78.57	97.52	95.67	77.08	98.14	96.01
14	86.63	97.18	95.74	88.88	96.68	96.10
15	86.43	96.54	96.13	83.45	97.36	96.32
16	83.36	97.55	96.27	84.49	97.74	96.61
17	83.19	96.13	95.04	88.45	96.22	95.64
18	86.27	96.57	95.75	83.73	97.98	96.67
19	89.67	97.33	96.69	81.06	98.55	96.81
20	88.23	96.77	96.14	78.69	98.09	96.29
AVG	82.80	97.16	95.88	84.02	97.49	96.33

maximum Gabor Wavelet responses and Local Binary Pattern (LBP). Fraz et al. [2] presented another approach for retinal blood vessels segmentation based on supervised classification using ensemble classifier of boosted and bagged decision trees. Method was tested on DRIVE, STARE and CHASE DB1 databases. This method also addressed the presence of pathological signs in their segmentation but it couldn't perform well in the severe cases of diseases. Wang et al. [11] came up with a supervised hybrid approach for vessel segmentation. Trainable Hierarchical Feature Extraction using Convolutional Neural Network (CNN) classifier was performed. Random Forests (RFs) trainable classifier with the 'winner-takes-all' technique was employed to categorize pixels into vessels and non-vessels. Method was evaluated on STARE and DRIVE databases. The main drawback of this method is that it couldn't perform efficient segmentation and missed some small vessel segments. Artificial Bee Colony (ABC) based segmentation technique optimized with fuzzy c-means clustering (FCM) was presented in [12]. Proposed approach consisted of two levels, at first level ABC optimization is applied using FCM objective function to localize vessels. At second level, acquired clusters are enhanced using pattern search approach to localize small thin vessels. This method was evaluated on the pathological retinal images but they still produce false positives due to poor segmentation. Asad et al. [13] proposed water flooding based retina blood vessel segmentation imitated by the concept of water flooding over land. Segmentation based on water flooding assumes that water always goes towards low land under the effect of gravity. Proposed algorithm is applied on DRIVE database which only contains healthy images and it didn't cater pathological retinal images in their implementation. A new method for retinal blood vessel segmentation with the combination of two methods of histogram maximum and minimum points and mathematical morphology was presented in [14]. The method was tested on DRIVE dataset only. Nyuyen et al. [15] presented an effective approach for vessel segmentation from color retinal image. It was based on the linear combination of line detector responses at varying scales. Method was tested on DRIVE, STARE and REVIEW databases. Phase Congruency and Histogram Clustering based segmentation of Retinal Vascular tree was introduced by Tagore et al. [16]. Phase Congruency technique was employed to enhance retinal images. Hierarchical clustering based histogram thresholding was used for blood vessels segmentation. This method performed comparatively better in the images with bright pathologies but couldn't perform

well in the presence of other pathological effects. Another method using gray level co occurrence based features was recently presented in [17]. They have used spatial structural information of fundus images to extract features along with neural networks for classification. They tested their method on DRIVE and STARE databases.

Later in the near past, a great emphasis has been made on the extraction of vascular pattern in the presence of different pathological signs but still there are many gaps which are required to be filled. Literature provides different methods in this context, some of them are summarized here. Shruthi et al. [18] presented an algorithm for the early detection of DR. Top-Hat and Bottom-Hat operations based method and K-means clustering were used to detect the retinal features. Finally K-NN classifier was used to perform the classification of retinal images. Akram et al. [19] presented an improved computer aided diagnosis system for early detection and grading of PDR. Vascular patterns were extracted by using Gabor wavelet and multi-layered thresholding. Multimodal m-Mediods based classifier was used to categorizes each vessel segment as normal or abnormal vessel. The validity of this system was tested on different databases of STARE, DRIVE, DIARETDB and MESSIDOR. Recently, an improved approach for blood vessels segmentation using Morphological Component Analysis (MCA) was presented in [20]. The main contribution of this paper is to separate lesions from vessels by selecting appropriate transforms. Morlet transform and adaptive thresholding were implemented to get final vessel map. The proposed system was evaluated on STARE and DRIVE databases. The drawback of this approach is removal of small vessels along with the fragmented vessel segments. Ganjee et al. [21] have proposed a method for vessel segmentation from pathological images. They proposed a two stage feature extraction technique for segmentation of vessels and removal of false regions. The evaluation was done on STARE database only. Table 1 summarizes the literature discussed in this section. It is clear from the literature that most of the work in the context of vessel segmentation has been done on healthy images. Presence of lesions and other pathological signs have hardly been considered in previous work [2, 3], [8–17]. The major drawback of existing state-of-art techniques is that they produce false positives when applied on unhealthy images. To address this issue we propose a robust algorithm for vessel segmentation

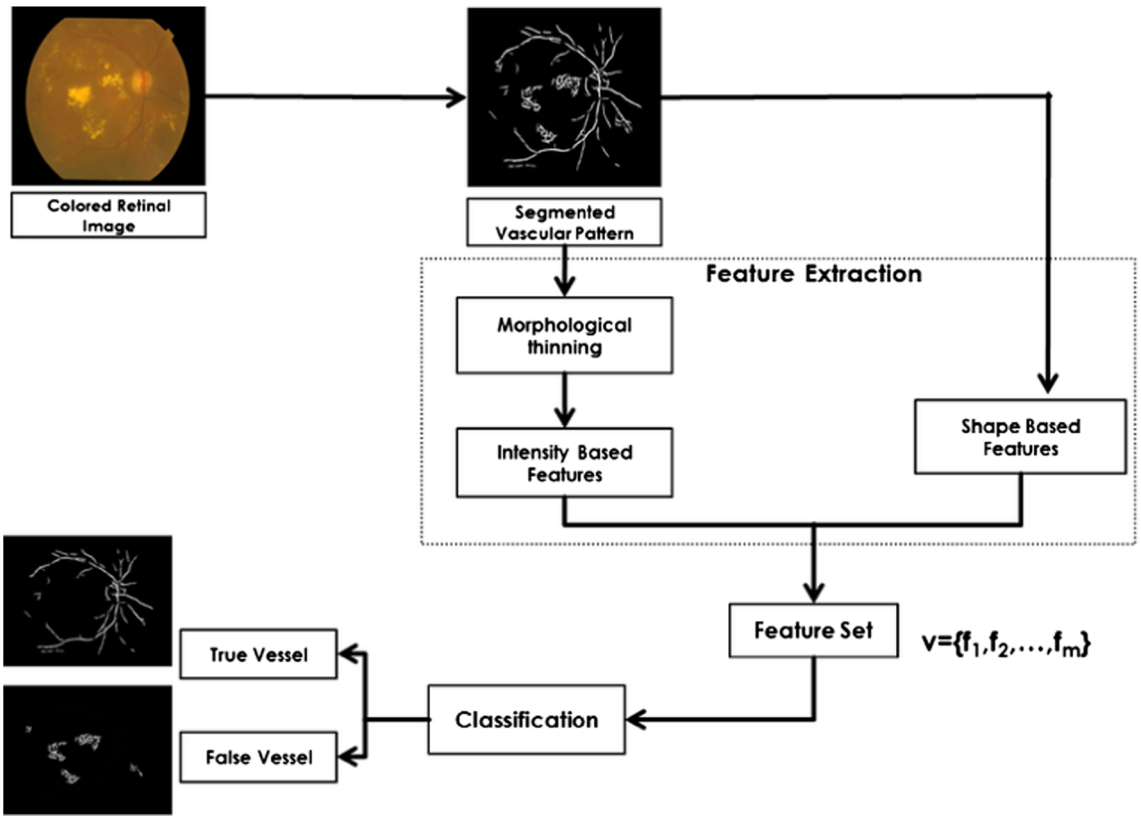

Fig. 2 Proposed System Overview

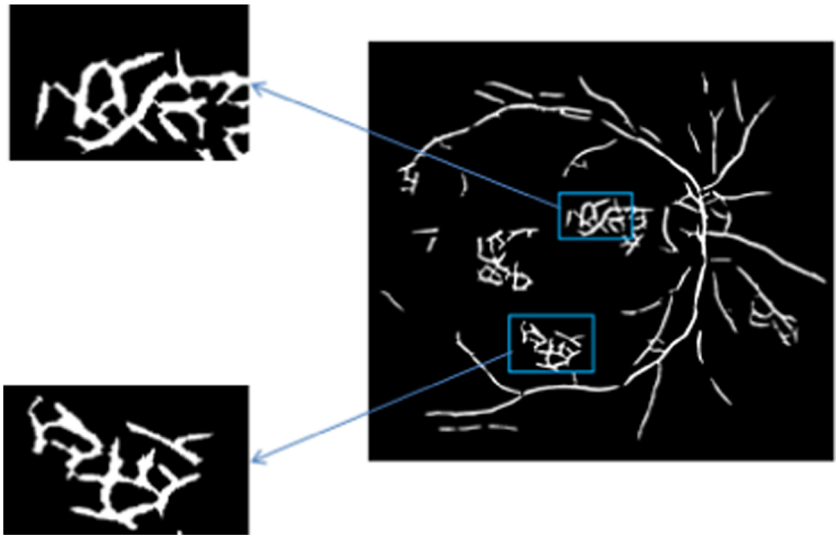

Fig. 3 Illustration of true and false vessels in the vascular pattern of diseased retinal image

with capability of handling severe stages of retinal diseases where more lesions and other pathological signs are present.

Proposed method

Automatic vessel segmentation serves many purposes in computer aided diagnosis systems for screening of ocular diseases. Segmentation of blood vessels in the presence of lesions and other artifacts is a very challenging task as discussed in Section "Introduction". To address this issue, this paper presents a robust algorithm for vessel segmentation even in the severe stages of ocular diseases. Figure 2 illustrates the flow diagram of proposed method. The proposed method intends to improve segmentation method reported in [22]. Region based feature extraction is performed based on the morphological characteristics and intensity values of true and false vessels. Afterwards, m-mediods based classifier is used to categorize retinal vascular regions into true vessels and false vessels.

Vessel segmentation

This step takes color retinal image as an input and extracts vascular pattern using multi-layered thresholding technique discussed in [22]. In the case of diseased retinal images extracted vascular patterns have lesions and exudates in the form of bunches and holes. During the screening through computer aided diagnosis systems, these false structures appear as false positives, which degrades the performance of overall system. Therefore, this paper attempts to improve [22] by removing the effects of lesions in the vascular pattern. The extracted vascular pattern obtained after applying technique in [22] are used in next step to cater false structures very precisely.

Shape and intensity based features extraction

In this step, different shape and intensity based features are extracted from the segmented vascular pattern. Presence of lesions in diseased retinal images gives rise to the growth of false vessels along with true vessels. True and false vessels have different morphological characteristics. Normal vessels appear in elongated shape with no holes and bunches, however false vessels appear as bunches and holes during automated detection as illustrated in Fig. 3.

This step first extracts candidate regions through connected component analysis and consider each connected segment in vessel map as a region. For each candidate region a feature set is formulated. If a retinal image I has n candidate regions, then feature set representation for an image I is $I = \{v_1, v_2, \ldots, v_n\}$, where v_j is a feature vector for j^{th} candidate region containing m features as $v = \{f_1, f_2, \ldots, f_m\}$. Particularly, this method extracts seven different features based on the morphological properties and intensity values of true and false vessels. Figure 4 shows a flow diagram for extraction of intensity based features. It used thinned vessels containing centerlines for actual vessel to extract these features.

Description of the extracted features is given below:

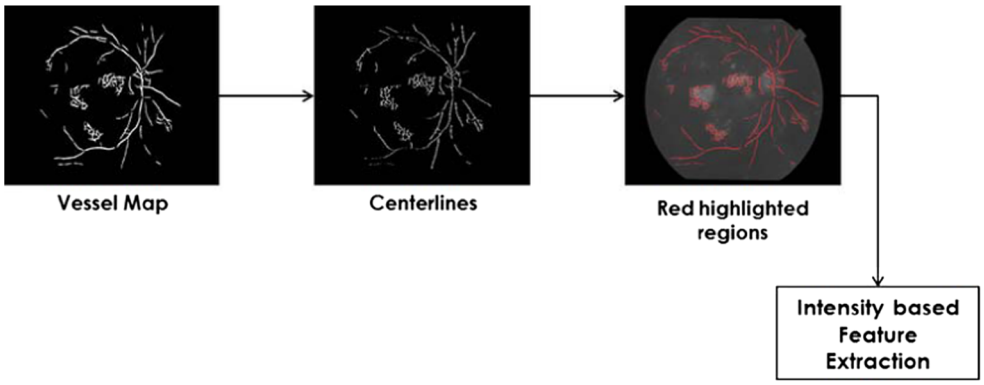

Fig. 4 Flow diagram showing steps for intensity based feature extraction

1. Extent (f_1): It is defined as the ratio of pixels in the region to pixels in the total bounding box. This feature has low value for true vessel segment as compared to false vessel segment.
1. MajorAxisLength(f_2): It reflects length of major axis of the ellipse. As true vessels are thin and elongated in shape, while false vessel segments appear as fragmented bunches, so value of major axis length for true vessels is high than false vessels.
2. ConvexArea (f_3): It is the number of pixels in convex image. This feature has high value for false vessel segments.
3. FilledArea(f_4): It shows number of pixels in the filled image. This feature has high value for false vessel segments as they appear in the form of circular bunches and they show more number of pixels in unit area than elongated true vessels.
4. Solidity(f_5): Shows proportion of pixels in the convex hull that are also in the region. False vessels cover more number of pixels in the convex hull, so this feature is more discriminating for false vessels as compared to true ones.
5. MinIntensity(f_6): This feature identifies the value of pixel with lowest intensity in the particular region. False structures like dark lesions and dark exudates have less intensity values, so this feature has high value for such pathological signs.
6. MeanIntensity (f_7): This specifies mean of all intensity values in the particular region. This feature shows high value for the false vessels appearing as filled holes and bunches with uniform intensity values.

Classification

The given 7-dimensional feature space representation of regions is enhanced using Localized Fisher Discriminant Analysis (LFDA) which enhances the feature space by minimizing the intra-class separations whilst maximizing the inter-class distance. Let $DB = \{F_1, F_2, .., F_n\}$ represents a set of n training samples belonging to true and false vessel region classes. The between class and within class scatter matrix is calculated using:

$$\Im_b = \frac{1}{2}\sum_{i=1}^{n}\sum_{j=1}^{n} W_{i,j}^{b}(\|F_i, F_j\|) \tag{1}$$

$$\Im_w = \frac{1}{2}\sum_{i=1}^{n}\sum_{j=1}^{n} W_{i,j}^{w}(\|F_i, F_j\|) \tag{2}$$

where $\|.,.\|$ is a Euclidean distance function and

$$W_{i,j}^{w} = \begin{cases} exp\left(\frac{\|F_i,F_j\|^2}{\wp_i\wp_j}\right) * \frac{1}{n_k} & iff \;\; F_i \wedge F_j \in \mathbf{L_k} \\ 0 & otherwise \end{cases} \tag{3}$$

$$W_{i,j}^{b} = \begin{cases} exp\left(\frac{\|F_i,F_j\|^2}{\wp_i\wp_j}\right) * \left(\frac{1}{n} - \frac{1}{n_k}\right) & iff \;\; F_i \wedge F_j \in \mathbf{L_k} \\ \frac{1}{n} & otherwise \end{cases} \tag{4}$$

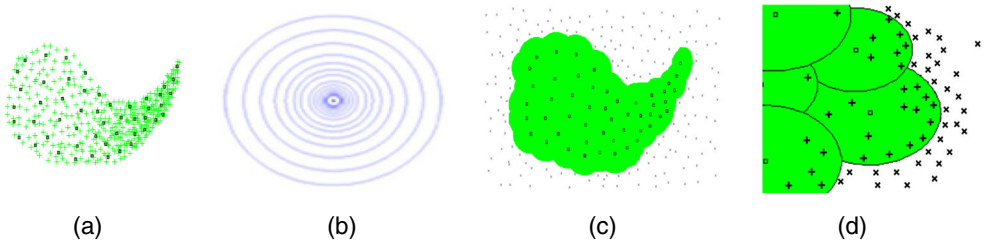

Fig. 5 Depiction of proposed m-Mediods based modeling and classification approach (**a**) Identification of m-Mediods (**b**) Computation of possible normality ranges (**c**) Detection of customized normality range for each mediod (**d**) Classification of regions into true and false vessel regions

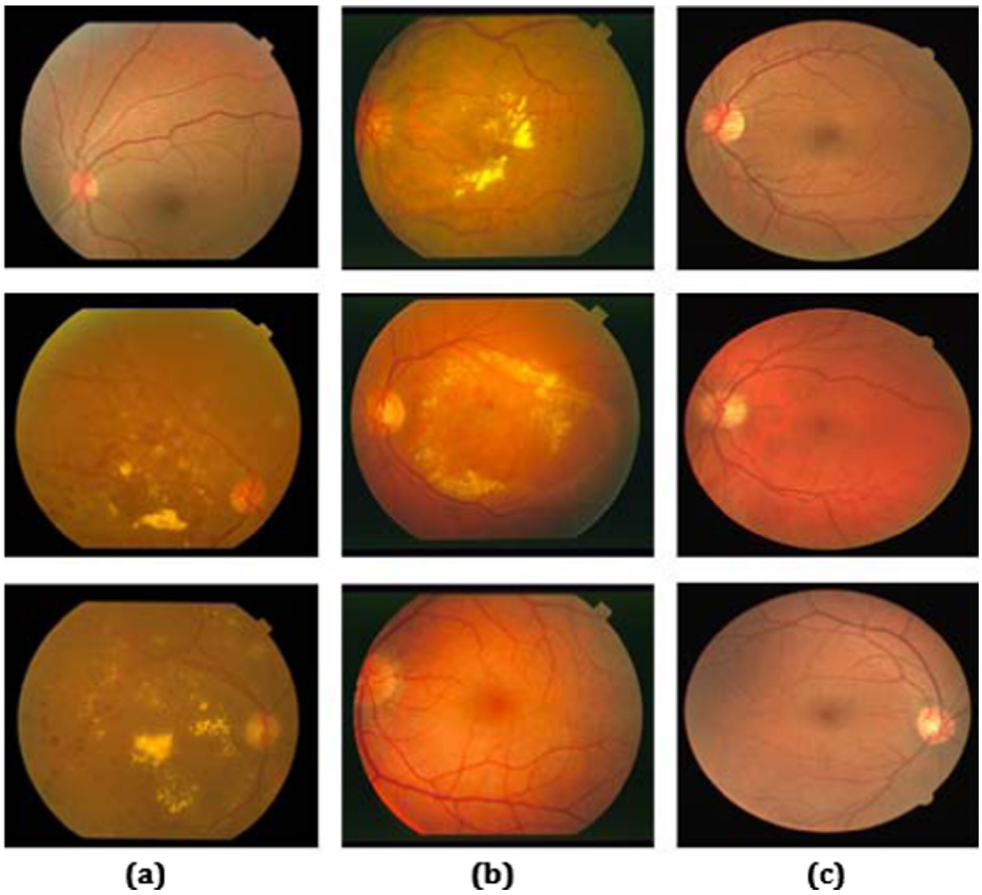

Fig. 6 Databases **a**) AFIO **b**) STARE **c**) DRIVE

Here, n_k is the membership count of class $\mathbf{L_k}$ and $\wp_i$ is the average distance of sample F_i with its k nearest neighbors. The LFDA based coefficient space representation is generated by performing generalized eigenvalue decomposition of $\Im_b E = \lambda \Im_w E$ where λ is a generalized eigenvalue and E is the corresponding eigenvector. The enhanced feature space representation of lesion ($\widetilde{F}$), using localized Fisher discriminant directions, is obtained as:

$$\widetilde{F} = \{E_1, E_2, .., E_m\} \tag{5}$$

where $\{E_1, E_2, .., E_m\}$ are eignevectors arranged in descending order w.r.t. their corresponding eigenvalues $\{\lambda_1, \lambda_2, .., \lambda_m\}$.

The enhanced feature space representation of regions is modeled using an extension of multivariate m-Mediods classifier as employed in [23]. We employ m-Mediods based classification by refining it for a given one-class classification problem. The presented approach comprises of three main steps: (i) Identification of m-Mediods for a given vessel class (ii) Detection of normality range for each mediod to separate true vessel class from false vessel class (iii) Classification of regions into one representing true vessels or false vessels. The mediod based learning and classification proposed in this paper is the one class classifier framework using m-Mediods model which is the extension of the multi class m-Mediods classification framework [24]. The problem at hand ideally suits one class classification where we have normal vessels and those that deviate significantly from normal vessel class as false/abnormal vessels. The extended one-class classification algorithm using m-Mediods model adapts nicely to the problem at hand.

Mediods for a given class is computed by employing Hierarchical Semi-Agglomerative approach (HSACT). This is achieved by identifying larger number of tiny clusters then the desired number of mediods from the samples belonging to a given class. We utilized Learning Vector Quantization (LVQ) to identify desired number of cluster centers. It has been shown in our previous work [25] that clustering using hierarchical semi-agglomerative approach employing a neural network, such as HSACT-LVQ, outperforms hard clustering techniques such as k-Means whilst performing faster than other neural network flavors such as self

Table 3 Image wise vessel segmentation results for STARE database

	OBSERVER 1			OBSERVER 2		
IMG	TPR	TNR	ACC	TPR	TNR	ACC
1	73.61	97.73	95.80	74.94	96.16	94.20
2	72.80	97.10	95.48	81.78	93.77	93.11
3	86.65	96.81	96.21	79.64	92.69	91.93
4	69.85	88.95	87.54	83.60	86.67	86.44
5	73.57	96.36	94.30	76.20	94.90	92.94
6	87.10	96.66	96.00	74.49	96.31	93.82
7	79.17	98.74	97.17	75.85	98.03	95.15
8	84.36	97.95	96.93	69.96	98.45	94.54
9	77.76	99.02	97.35	74.96	97.65	94.87
10	83.35	97.32	96.20	65.05	97.73	92.74
11	77.19	98.36	96.85	72.74	97.84	94.97
12	75.35	98.96	97.14	79.66	98.62	96.43
13	82.09	98.45	96.99	72.74	97.84	94.97
14	81.87	98.57	97.06	73.80	98.88	95.55
15	78.59	97.62	95.97	77.81	98.01	95.48
16	63.04	98.43	94.82	61.53	98.34	92.73
17	70.27	99.28	96.68	68.35	98.87	94.87
18	79.09	98.83	97.84	80.85	98.05	96.99
19	85.22	97.41	96.89	81.02	96.32	95.36
20	75.12	96.50	95.08	71.97	95.20	92.89
AVG	77.80	97.45	95.91	74.82	96.58	94.01

organizing maps (SOM). Let $\mathbf{C}$ be the set of cluster centers identified using feature vector representation of regions from true vessel class, the desired number of cluster centers (m) is obtained by merging the closest pair of cluster centers, employing weighted mean mechanism, as

$$C_{ab} = \frac{|C_a| \times C_a + |C_b| \times C_b}{|C_a| + |C_b|} \tag{6}$$

where (a, b) are the index of closest pair of cluster centers and $|.|$ is the membership count function. The closest pair of cluster centers are identified as:

$$(a, b) = arg\,min_{(i,j)}\ [(C_i - C_j)^T (C_i - C_j)]^{\frac{1}{2}} \quad \forall i, j \wedge i \neq j \tag{7}$$

The distance between two cluster centers is scaled by their membership counts to encourage more cluster centers and in turn mediods, in regions with high density of samples and vice versa. This is critical for catering multivariate and nonlinear data distributions. The process of merging of closest pair of cluster centers continues till the number of cluster centers gets equal to the desired number of mediods to model a given class. The resultant set of mediods $\mathbf{C}$ is then employed to identify the normality range for each mediod in $\mathbf{C}$. This is achieved by first identifying the set of possible normality ranges $\mathbf{R}$ which is accomplished by computing the distance between each pair of mediods belonging to $\mathbf{C}$. The identified set of ranges $\mathbf{R}$ is then employed to identify normality range separately for each mediod. We select that normality range from the set $\mathbf{R}$ which results in maximum number of samples from true vessel class to fall in the normality range of the mediods modeling regions containing true vessels whilst letting minimum number of samples from false vessel class. This in turns become an optimization problem to identify the customized normality range for each mediod that minimizes false positives and false negatives.

After the identification of mediods and their corresponding normality ranges, the classification of feature space representation of vessel regions $\widetilde{F}$ is achieved by computing the k nearest mediods $k - NM$ w.r.t. $\widetilde{F}$ using

$$k - NM(\widetilde{F}, \mathbf{C}, k) = \{\mathbf{P} \in \mathbf{C} | \forall X \in \mathbf{P}, Y \in \mathbf{C} - \mathbf{P}, \\ \|\widetilde{F}, X\| \leq \|\widetilde{F}, Y\| \wedge |\mathbf{P}| = k\} \tag{8}$$

where $\mathbf{C}$ is the set of all cluster centers representing mediods, $\mathbf{P}$ is the set of k closest cluster centers and

$\|.,.\|$ is the euclidean distance function. The region, represented by its feature vector $\widetilde{F}$, is classified as true vessel region if it lies within the normality range of one of the k nearest mediods. Otherwise, the region is classified as false vessel region. The depiction of proposed m-Mediods based modeling and classification approach is presented in Fig. 5. Figure 5(a) depicts the identification of mediods, represented by squares, given the feature space representation of true vessel regions, represented by '+' markers. The possible normality ranges extracted based on the inter-mediod distances is presented in Fig. 5(b). Figure 5(c) shows the identification of the customized normality ranges for the mediods representing true vessel classes. The normality range is identified such that the feature space representation of true vessel classes falls within the normality range of the mediods whilst rejecting the false vessel regions, represented by 'x' marker. Figure 5(d) depicts the classification using the learned m-Mediods model. The feature space representation of regions falling within the normality range of mediods (represented by '+' marker) are classified as true vessel regions where the regions falling outside the normality ranges (represnted by 'x' marker) are classified as false vessel regions.

Experimental results

Database

Proposed system is assessed on three databases, two publicly available databases DRIVE and STARE and third own database of AFIO. There are 40 fundus images in DRIVE, out of which 7 are diseased images and 33 are healthy images [26]. Images are taken digitally from a Cannon CR5 3CCD camera with 45 degree FOV. Each image has a resolution of 768x584 pixels and compressed in JPEG format. DRIVE dataset is divided into two sets; the training set and the test set where each set contains 20 images. For comparison purpose, the performance of the proposed method is measured on 20 test images. STARE has total 20 images and 10 of them are diseased images [27]. These images are acquired by a Topcon TRV-50 fundus camera. Each image is of 605x700 pixels resolution and stored in PPM format. AFIO dataset consists of 462 total images including 160 healthy images and 302 diseased images with the resolution of 1504x1000 pixels. Images are captured by Topcon 50EX with 30 degree FOV. Each image is stored in JPEG format. Some of the images of all databases used in the proposed system are shown in Fig. 6.

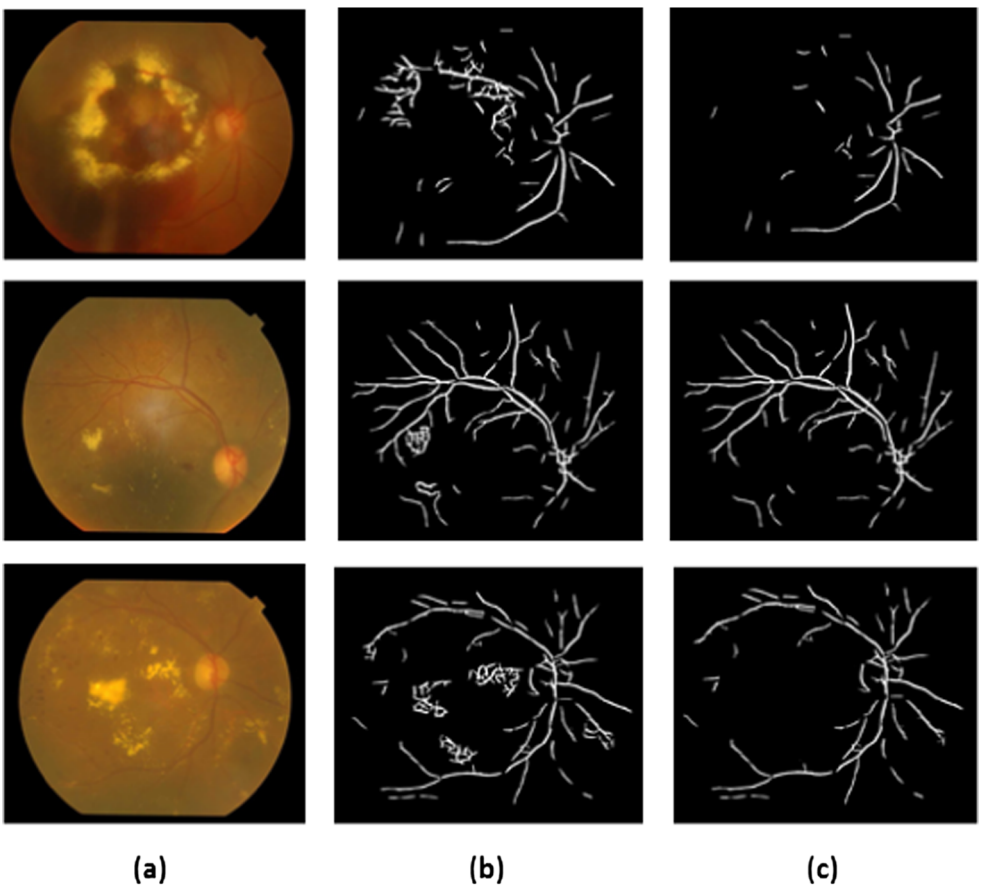

Fig. 7 **a**) Color fundus image (from AFIO database) **b**) Segmented Blood Vessels of Images in (**a**). **c**) Final Output of Proposed Method (without false vessels)

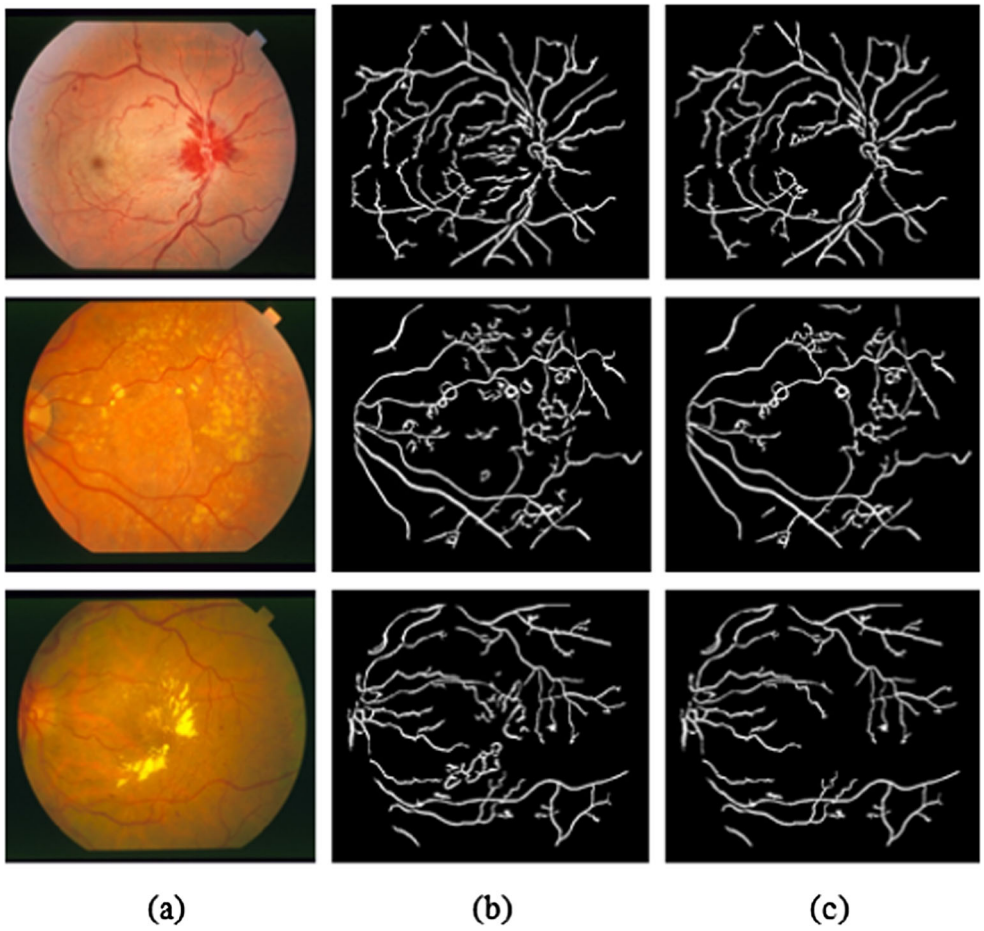

Fig. 8 **a**) Color fundus image (from STARE database) **b**) Segmented Blood Vessels of Images in (**a**). **c**) Final Output of Proposed Method (without false vessels)

Performance measures

The evaluation of proposed system is done using performance measures i.e. Accuracy, Sensitivity and Specificity which are calculated by using equations 9-11.

$$Sensitivity(TPR) = \frac{T_P}{T_P + F_N} \tag{9}$$

$$Specificity(TNR) = \frac{T_N}{T_N + F_P} \tag{10}$$

$$Accuracy = \frac{T_P + T_N}{T_P + T_N + F_N + F_P} \tag{11}$$

Where,

- T_P (True Positive) represents the number of true vessel regions correctly classified as true vessels.
- F_P (False Positive) represents the number of false vessel regions classified as true vessels.
- T_N (True Negative) represents the number of false vessel regions correctly classified as false vessels.
- F_N (False Negative) represents the number of true vessels classified as false vessels.

Results analysis

Proposed method is tested on three databases DRIVE, STARE and AFIO. Table 2 shows the resulted performance measures values after applying the proposed algorithm on the test set consisting of 20 images in the DRIVE database. Two manual segmentations by two different observers are used as the ground truth for the evaluation of 20 test images in DRIVE database. Average results are shown in bold fonts.

Similarly, Table 3 shows the detailed results for 20 images of STARE database. All images are evaluated against the two manually segmented results. Average results are shown in bold fonts.

Table 4 illustrates the comparison between the performance of proposed algorithm and performances of the state-of-art algorithms on DRIVE and STARE databases where the empty cells are not reported by their authors. Comparison clearly shows the robustness of proposed method in terms of improved performance measures values.

Pictorial results of proposed system for AFIO dataset are shown in Fig. 7. Column (a) shows color diseased fundus images, Column (b) shows vessel maps of images in (a) extracted through segmentation method reported in [22]

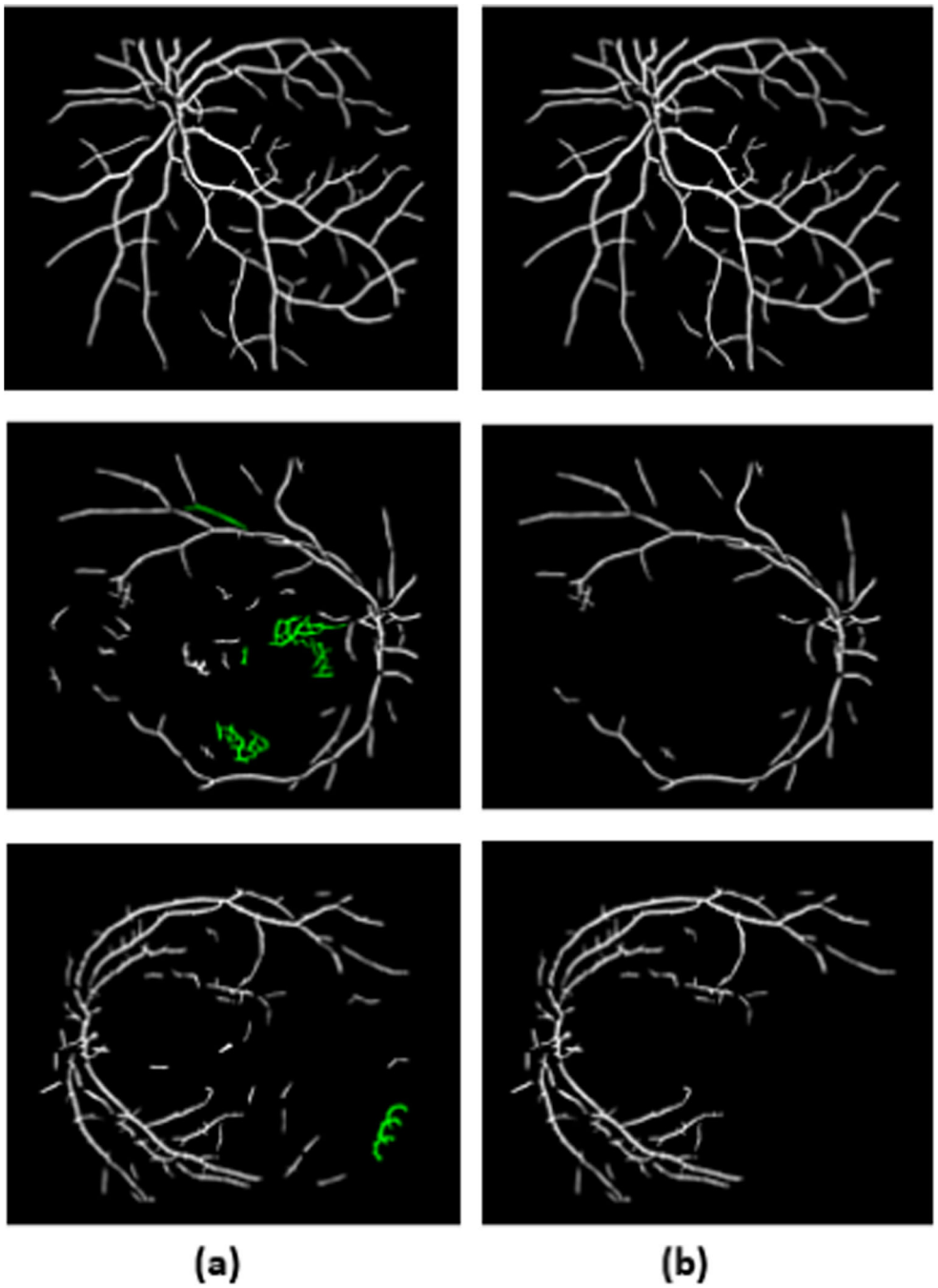

Fig. 9 **a**) Results of method [22] **b**) Results of proposed method

which includes both true and false vessels and Column (c) shows the final output of the proposed system showing vessel maps of images in (a) which are without false vessels. So, final output of the proposed method clearly depicts the effectiveness of proposed algorithm in removing false positives from the diseased image vasculature. Similarly, pictorial results for STARE dataset are shown in Fig. 8.

Figure 9 shows the results comparison of our proposed method with that of segmentation technique discussed in [22]. Column (a) shows results of segmentation technique reported in [22] and Column (b) shows results of our proposed method. First image is the healthy retinal image and rest two images are diseased retinal images. It is evident from the results that outputs of method [22] (in (a)) have false positives which are represented in green pixels, while results of our proposed method (in (b)) have no false positives. So, the proposed method significantly removes false positives in its final outputs.

Figure 10 shows comparison of proposed method results with manually marked results for DRIVE and STARE. White pixels depict true vessels, green pixels depict false

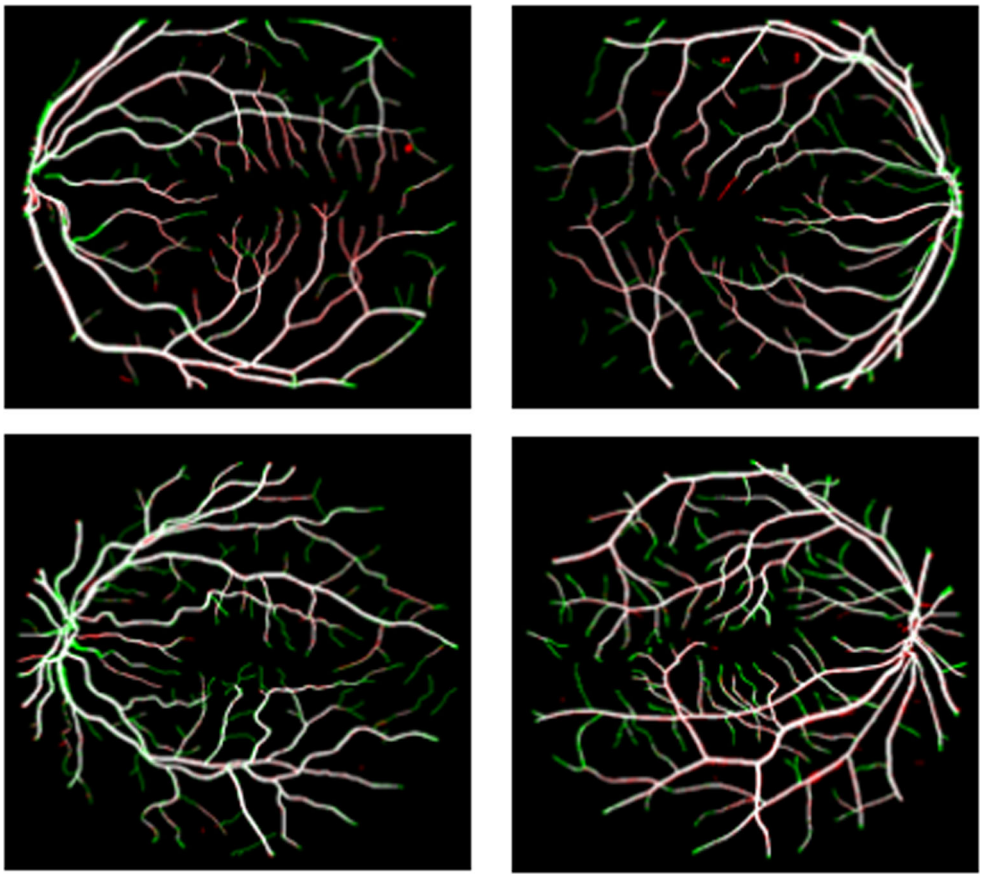

Fig. 10 Comparison of proposed method results with the manually marked results Row1) for STARE Row2) for DRIVE

positives and red pixels depict false negatives. Here false positives are the pixels which are detected as vessels by the proposed system but they are actually non vascular pixels similarly false negatives are those pixels which are detected as non vascular pixels by the proposed system but they are actually vascular pixels. Proposed method results greatly reduce false positives and false negatives in the final output.

Table 5 shows evaluation of proposed method on DRIVE, STARE and AFIO datasets. DRIVE and STARE datasets have high values of accuracies as compared to AFIO dataset

Table 4 Comparison of proposed system with existing state of the art on DRIVE and STARE databases

	DRIVE			STARE		
Methods	TPR	TNR	Accuracy	TPR	TNR	Accuracy
Emray et al. [12]	72.1	97.1	93.9	64.9	98.2	94.7
Aramesh et al. [14]	78.4	98.26	94.8	–	–	–
Imani et al. [20]	75.82	97.48	95.25	75	97.31	95.75
Tagore et al. [16]	–	–	94.24	–	–	94.97
Asad et al. [13]	62.92	98.21	93.69	–	–	–
Akram et al. [22]	–	–	94.69	–	–	95.02
Soares et al. [8]	–	–	94.66	–	–	94.80
Nguyen et al. [15]	–	–	94.07	–	–	93.24
Proposed Method (SVM)	79.37	97.79	96.16	80.70	97.10	95.81
Proposed Method (observer-1)	82.80	97.16	95.88	77.80	97.45	95.91
Proposed Method (observer-2)	84.02	97.49	96.33	74.82	96.58	94.01

Table 5 Evaluation of Proposed Method on all databases

Database	Total Images	Healthy	Diseased	TPR (%)	TNR (%)	ACC (%)
DRIVE	40	33	7	84.02	97.49	96.33
STARE	20	10	10	77.80	97.45	95.91
AFIO	462	160	302	86.20	95.04	91.98

because AFIO dataset has more diseased images than other two datasets.

Conclusion

Blood vessels are the most important retinal features which can noticeably be effected by many worldwide diseases like diabetes, hypertension etc. Any change in the peculiar properties of these vessels can serve as an indicator for diagnosis of many eye diseases. These diseases are diagnosed by performing an automated retinal image analysis. Blood vessels segmentation is the major step in an automated retinal image analysis. Inclusion of different abnormalities due to diseases makes blood vessel segmentation a very challenging task. This paper presented a robust algorithm which performs region based analysis to extract true vessels and false vessels from diseased fundus images. The proposed technique is tested on AFIO, STARE and DRIVE databases. It is evident from the experimental results that the proposed method outperforms the existing state-of-art techniques on vessel segmentation from diseased fundus images. The proposed method will be helpful in reliable person's recognition by using the output vascular patterns.

Acknowledgment This research is funded by National ICT R&D fund, Pakistan. We are also thankful to Armed Forces Institute of Ophthalmology (AFIO) for their clinical support and help.

Conflict of interests The authors declare that there is no conflict of interests regarding the publication of this manuscript.

References

1. Rozlan, A.Z., Hashim, H., Farid, S., Adnan, S., Hong, C.A.: A proposed diabetic retinopathy classification algorithm with statistical inference of exudates detection, 2013 International Conference on Electrical, Electronics and System Engineering, 2013.
2. Fraz, M.M., Remangnino, P., Hoppe, A., Uyyanonvara, B., Rudnicka, A.R., Owen, C.G., Barman, S.A., An ensemble classification-based approach applied to retinal blood vessels segmentation. *IEEE Trans. Biomed. Eng.* 59(9), 2012.
3. Fraz, M.M., Remagnino, P., Hoppe, A., Velastin, S., Uyyanonvara, B., Barman, S.A.: A supervised method for retinal blood vessel segmentation using line strength, multiscale gabor and morphological features, IEEE International Conference on Signal and image Processing Applications (ICSIPA), 2011.
4. Akram, U.M., and Khan, S.A., Automated detection of bright and dark lesions in retinal images for early detection of diabetic retinopathy. *J. Med. Syst.* 36(5), 2011.
5. MerckManuals, www.merckmanuals.com/professional/eye_disorders/retinal_disorders/hypertensive_retinopathy.html Last Accessed on 21st October, 2014.
6. Grisan, E., and Ruggeri, A.: Segmentation of Candidate Dark Lesions in Fundus Images based on Local thresholding and Pixel Density, 29th Annual Conference of IEEE, Engineering in Medicine and Biology Society (EMBS), Lycon 22-26 Aug, 2007.
7. Zhang, Z., Srivastava, R., Liu, H., Chen, X., Duan, L., Wong, D.W.K., Kwoh, C.K., Wong, T.Y., Liu, J., A survey on computer aided diagnosis for ocular diseases. *BMC Med. Inf. Decis. Making* 14(1):80, 2014.
8. Soares, J.V.B., Leandro, J.J.G., Cesar, R.M., Jelinek, H.F., Cree, M.J.: Retinal vessel segmentation using the 2-d Gabor wavelet and supervised classification, Medical Imaging, IEEE Transactions, 2006.
9. Raja, D.S.S., Vasuki, Dr.S., Kumar, Dr.R., Performance analysis of retinal image blood vessels segmentation. *Adv. Comput. An Int. J. (ACIJ)* 5(2/3), 2014.
10. Holbura, C., Gordan, M., Vlaicu, A., Stoian, L., Capatana, D.: Retinal vessels segmentation using supervised classifiers decisions fusion. Automation quality and testing robotics (AQTR), IEEE International Conference, 24-27 May, 2012.
11. Wang, S., Yin, Y., Cao, G., Wei, B., Zheng, Y., Yang, G.: Hierarchical retinal blood vessel segmentation based on feature and ensemble learning, Neurocomputng, Vol.149, 2015.
12. Emary, E., Zawbaa, H.M., Hassanien, A.E., Schaefer, G., Ahmad, T.A.: Retinal blood vessel segmentation using artificial bee colony optimisation and pattern search, 2014 International joint conference on neural networks (IJCNN), Beijing China, July 6–11, 2014.
13. Asad, A.H., Elamry, E., Hassanein, A.El.: Retinal vessels segmentation based on water flooding model, 9th International computer engineering conference (ICENCO), 28-29 December, 2013.
14. Aramesh, R., and Faez, K., A new method for segmentation of retinal blood vessels using Morphological image processing technique. *Int. Learn. Adv. Stud. Comput. Sci. Eng. (IJASCSE)* 3(1), 2014.
15. Nguyen, U.T.V., Bhuiyan, A., Park, L.A.F., Ramamohanarao, K., An effective retinal blood vessel segmentation method using multi-scale line detection. *Pattern Recogn.* 46(3):703–715, 2013.
16. Tagore, M.R.N., Kande, Dr.G.B., Rao, Dr.E.V.K., Rao, Dr.B.P.: Segmentation of retinal vasculature using phase congruency and hierarchical clustering, IEEE 2013 International Conference on Advances in Computing, Communications and Informatics (ICACCI),22-25 August, 2013.
17. Javad, R., and Hardala, F., Retinal blood vessel segmentation with neural network by using gray-level co-occurrence matrix-based features. *J. Med. Syst.* 38(8):1–12, 2014.
18. Shruthi, C. H., Ramakrishna, N., Muthukrishnan, Dr.N.M., Detection and classification of diabetic retinopathy condition in retinal images. *Int. J. Innovative Research Electron. Commun. (IJIREC)* 1(6), 2014.
19. Akram, M.U., Khalid, S., Tariq, A., Javed, M.Y., Detection of neovascularization in retinal images using multivariate m-mediods based classifier. *Comput. Med. Imaging Graphics (2013)* 37(5-6), 2013.
20. Imani, E., Javidi, M., Pourreza, H.R., Improvement of retinal blood vessel detection using morphological component analysis. *Comput. Methods Prog. Biomed.* 118(3), 2015.

21. Ganjee, R., Azmi, R., Gholizadeh, B., An improved retinal vessel segmentation method based on high level features for pathological images. *J. Med. Syst.* 38(9):1–9, 2014.
22. Akram, M.U., and Khan, S.A., Multilayered thresholding-based blood vessel segmentation for screening of diabetic retinopathy. *Engineering with computers* 29:165–173, 2013.
23. Bashir, F.I., Khokhar, A.A., Schonfeld, D., View-invariant motion trajectory based activity classification and recognition, ACM multimedia systems, special issue on machine learning approaches to multimedia information retrieval, 45–54, 2006.
24. Akram, M.U., Khalid, S., Khan, S.A., Identification and classification of microaneurysms for early detection of diabetic retinopathy. *Pattern Recog.* 46(1):107–116, 2013.
25. Khalid, S., and Razzaq, S., Frameworks for multivariate m-mediods based modeling and classification in Euclidean and general feature spaces. *Pattern Recog.* 45(3):1092–1103, 2012.
26. Staal, J., Abramoff, M.D., Niemeijer, M., Viergever, M.A., van Ginneken, B., Ridge-based vessel segmentation in color images of the retina. *IEEE Trans. Med. Imag.* 23:501–509, 2004.
27. Hoover, V.K., and Goldbaum, M., Locating blood vessels in retinal images by piecewise threshold probing of a matched filter response. *IEEE Trans. Med. Imag.* 19:203–211, 2000.